Fukuzawa *et al. Earth, Planets and Space* (2017) 69:54
DOI 10.1186/s40623-017-0638-y

Earth, Planets and Space

FULL PAPER

Open Access

Generation of billow-like wavy folds by fluidization at high temperature in Nojima fault gouge: microscopic and rock magnetic perspectives

Tomohiko Fukuzawa[1], Norihiro Nakamura[2*], Hirokuni Oda[3], Minoru Uehara[4] and Hiroyuki Nagahama[1]

Abstract

Microscopic billow-like wavy folds have been observed along slip planes of the Nojima active fault, southwest Japan. The folds are similar in form to Kelvin–Helmholtz (KH) instabilities occurring in fluids, which implies that the slip zone underwent "lubrication" such as frictional melting or fluidization of fault gouge materials. If the temperature range for generation of the billow-like wavy folds can be determined, we can constrain the physical properties of fault gouge materials during seismic slip. Here, we report on rock magnetic studies that identify seismic slip zones associated with the folds, and their temperature rises during ancient seismic slips of the Nojima active fault. Using a scanning magneto-impedance magnetic microscope and a scanning superconducting quantum interference device microscope, we observed surface stray magnetic field distributions over the folds, indicating that the folds and slip zones are strongly magnetized. This is due to the production of magnetite through thermal decomposition of antiferromagnetic or paramagnetic minerals in the gouge at temperatures over 350 °C. The presence of micrometer-sized finely comminuted materials in the billow-like wavy folds, along with our rock magnetic results, suggests that frictional heating-induced fluidization was the driving mechanism of faulting. We found that the existence of the magnetized KH-type billow-like wavy folds supports that the low-viscosity fluid induced by fluidization after frictional heating decreased the frictional strength of the fault slip zone.

Keywords: Rock magnetism, Nojima fault, Frictional heating, KH instability, MI magnetic microscope, Scanning SQUID microscope

Introduction

One of the only ways to identify a drastic decrease in the friction coefficient during seismic slip in outcrop is to measure the frictional heating on faults relative to the surrounding rock. Di Toro et al. (2011) indicated that the physical properties of fault gouge at seismic slip rates (about 1 m/s) cause a significant decrease in friction (of up to one order of magnitude), which we call fault "lubrication," lubrication reduces normal stress along the fault plane, being mainly caused by frictional melting (Jeffreys 1942; McKenzie and Brune 1972; Sibson 1975; Cardwell et al. 1978; Allen 1979), thermal pressurization (Sibson 1973; Lachenbruch 1980; Mase and Smith 1984, 1987), and/or fluidization (Monzawa and Otsuki 2003; Ujiie et al. 2007; Boullier et al. 2009) of the fault gouge. As these lubrication mechanisms might be recorded in fault gouge as microtextures, it is important to find direct evidence from natural gouge to evaluate ancient frictional faulting mechanisms.

It is known that Nojima fault gouge preserves a unique "billow-like wavy folds" microtexture produced during ancient seismic slip events at a seismogenic depth (Kameda et al. 2002; Otsuki et al. 2003). The wavy folds are similar to the Kelvin–Helmholtz (KH) instability that normally occurs in fluids (Helmholtz 1868; Kelvin 1871).

*Correspondence: n-naka@tohoku.ac.jp
[2] Institute for Excellence in Higher Education, Tohoku University, Sendai, Japan
Full list of author information is available at the end of the article

Such an instability is generated at the interface between two fluids of different densities that are shearing at different velocities. Each fold is inclined in shearing direction and tapers to the wave crest. The differing velocities cause a pressure difference due to the "Bernoulli effect," leading to the instability. Therefore, the billow-like wavy fold microtexture is an indicator that the fault slip zone underwent "lubrication."

Such lubrication textures have been reported from geological scale to microscopic scales. Brodsky et al. (2009) examined a series of outcrop-scale asymmetrical flow-like intrusions of ultrafine-grained fault rock on the exhumed Kodiak Island megathrust, Alaska, using a concept of gravitational (Rayleigh–Taylor) instability to reveal a coseismic slip velocity of the order of 10 cm/s. Wetzler et al. (2010) suggested that the various types of outcrop-scale deformations in the Lisan Formation, Israel, could be explained as the result of earthquake-triggered KH instability. These field investigations give no constraint of temperature conditions during the deformation. High-velocity experiments carried out by Mizoguchi et al. (2009) indicated that the microscopic-scale billow-like textures in Nojima fault gouge are characterized by folding and fluttering structures during a steady-state frictional weakening stage. Moreover, using numerical modeling based on temperature measurements close to the gouge layer, they showed that the microtextures were formed under a relatively low temperature of less than 400 °C. In contrast, Otsuki et al. (2003) suggested that local frictional melting in Nojima fault gouge caused a fluid-like microstructure such as billow-like fold, but that local fluidization may also occur, which contributed to decrease the friction coefficient of the fault slip zone. To determine which temperature conditions occurred during ancient natural faulting in the Nojima fault, we need to know a temperature rise in a slip zone by frictional heating during seismic slips.

In order to identify seismic slip zones and constrain the temperature rise in fault gouge during seismic slip, electron spin resonance (ESR) (Fukuchi 2003, 2012), biomarkers (Savage et al. 2014), vitrinite reflectance (Maekawa et al. 2014), and rock magnetism (Mishima et al. 2006) investigations have been conducted. The ESR and rock magnetism studies focus on the production of ferromagnetic minerals in the slip zone due to thermal decomposition of paramagnetic minerals by frictional heating. The production of magnetic minerals yields remanent magnetization under Earth's magnetic field that is a permanent magnetization resulting in magnetic minerals (Dunlop and Özdemir 1997). Therefore, magnetized slip zones can be regarded as a fossilized signature of frictional heating. This suggests that ESR and rock magnetic investigations have advantage for determining the temperature rise in fault gouge. To identify spatial distribution of frictionally heated slip zones, Fukuchi (2012) developed a scanning ESR microscopy technique with a 0.25 mm spatial resolution; however, such technique has not been applied to the billow-like wavy folds in Nojima fault gouge. Moreover, there is no application of scanning magnetic microscopies to the folds.

There are three possible explanations of why a fault slip zone has high remanent magnetization than its surroundings. First, ferrimagnetic minerals in the fault slip zone may acquire a thermal remanent magnetization (TRM) upon cooling (Piper and Poppleton 1988; Ferré et al. 2014). Second, earthquake lightning may constitute an additional magnetization process (Enomoto and Zheng 1998; Ferré et al. 2005). Third, a fault slip zone may acquire chemical remanent magnetization (CRM) due to neoformation of ferrimagnetic minerals by thermal decomposition during seismic slips (Nakamura et al. 2002; Fukuchi 2003; Fukuchi et al. 2005; Hirono et al. 2006; Chou et al. 2012); it can be explained that many kinds of antiferromagnetic or paramagnetic minerals are thermally decomposed into ferrimagnetic minerals. Fukuchi (2003) indicated that Nojima fault gouge contains antiferromagnetic minerals such as kaolinite or smectite that can be changed into ferrimagnetic minerals such as maghemite by thermal dehydration. Nojima fault gouge contains siderite ($FeCO_3$) (Enomoto and Zheng 1998), which thermally decomposes into magnetite with carbon dioxide at 470 °C under reducing conditions (French 1971). Mishima et al. (2009) showed that paramagnetic minerals such as siderite in Taiwan Chelungpu fault gouge changed into ferrimagnetic magnetite through thermal decomposition above about 400 °C. These studies imply that analysis of ferrimagnetic minerals contributes to identifying seismic slip zones and the reconstruction of their temperature history during fault slips. In Japan, a scanning magneto-impedance (MI) magnetic microscope and a scanning superconducting quantum interference device (SQUID) microscope (SSM) for room-temperature samples have been developed at Tohoku University (Uehara and Nakamura 2007) and the Geological Survey of Japan (GSJ) National Institute of Advanced Industrial Science and Technology (AIST) (Kawai et al. 2016; Oda et al. 2016), respectively. These lines of equipment can detect the surface stray magnetic field over a thin section with a spatial resolution of 0.4 and 0.10 mm, respectively. In this study, we use a scanning magnetic microscopy method to identify seismic slip zones and obtain the temperature rise distribution around the billow-like wavy fold microtextures of Nojima fault gouge during seismic slip.

Study area and sampling

The Nojima fault is an active fault in Japan, which strikes N20°E–N60°E, dips 75°–85° to the southeast, and forms a boundary between granites and siltstone of the Osaka Group made of sandy gravel bed layer (Yoshikawa 1973; Uda et al. 2001). The fault ruptured during the Hyogo-ken Nanbu (Kobe) earthquake in 1995 (*Mw.* 6.9 according to National Earthquake Information Center). The earthquake yielded composite surface right-lateral displacement of 1.2–1.6 m and vertical displacement of 0.5–0.8 m, with maximum surface displacement of 2.5 m (2.1 m right-lateral and 1.3 m vertical) observed in the central part of surface faults in Hirabayashi district (Awata et al. 1996).

In a project that was part of the Nojima Fault Zone Probe (Oshiman et al. 2001), we trenched the Hirabayashi outcrop, found laminated fault gouge zone, and collected oriented samples (Fig. 1a, b). The hanging wall comprises white-colored weathered granite, and the foot wall comprises Osaka group siltstone (Fig. 1c). The fault gouge is about 20 cm wide (Fig. 1c) and is composed of alternating thin layers of very fine-grained material including weathered cataclastic granite, and laminated cohesive blackish and incohesive grayish fault gouges (Fig. 1d, e). Furthermore, we found billow-like wavy folds within cohesive blackish gouge and also at the boundary between blackish gouge and weathered granite (Fig. 1d, e). A power rock saw with a diamond blade was used to cut the oriented fault gouge blocks after they were reinforced with non-magnetic dental cement. The trenched fault zone was oriented N45°E and dipped to 80°E.

Detailed observations suggest that the surface seismic slip of the 1995 Hyogo-ken Nanbu earthquake only occurred in the soft fault clay along western-side siltstone (Otsuki et al. 1997). In our study, we focused on the laminated fault gouge zone with microtextures adjacent to the weathered granite. Therefore, this fault gouge zone preserves the signature of the large earthquake events in the ancient time before the 1995 event. This is not the product of the 1995 event. The estimated formation depth of this gouge is 3 km according to the clay mineral stability field (Otsuki et al. 2003). The thin sections of the fault gouge zone were taken perpendicular to the laminae on the horizontal plane, because the rake of the striation is unknown. A typical thin section of the laminated fault rock is shown in Fig. 2a. The fault gouge consists of three parts, incohesive grayish gouges, cohesive blackish gouges, and weathered granites (Fig. 2a, d). The gouges display disordered microtextures with turbulent, laminated structures and billow-like wavy folds (Fig. 2a, d). The billow-like wavy folds are observed at the boundary between the weathered granites and cohesive blackish gouge (Fig. 2d) and also in the laminated microtextures (Fig. 1d; Additional file 1: Fig. S1).

To describe the configuration of the billow-like wavy folds, we defined the width (l) as the distance between the base of the billow-like wavy folds and the most upper part of the curved folds and wavelength (λ) as the distance along the base between the two minimum points (Fig. 2e). Each fold is inclined in the same direction and tapers to the wave crest. The fold inclination suggests the left-lateral orientation of the fault movement, implying the ancient slip sense and ancient stress field were different from the present those. The amplitude and wavelength of the billow-like wavy folds stemming from the same boundary are almost equal. The billow-like wavy folds in Nojima fault gouge are similar to the wavy folds induced by KH instability that were identified in Dead Sea sediments by Wetzler et al. (2010). We adopted Wetzler et al.'s (2010) approach of characterizing the folds by a power spectrum comprising amplitude squared (l^2) and the inverse of wavelength ($k = 1/\lambda$), as shown in Fig. 3. We plotted l^2 and k for the billow-like wavy folds in Nojima fault gouge with those from the Dead Sea sediment deformations compiled by Wetzler (2009). The power spectrum ($l^2 = 0.15\ k^{-1.9}$) has a similar trend with a power law fit of -1.9 and correlation coefficient (R^2) of 0.98 (Fig. 3). This differs from the exponent of $-5/3$ which is predicted from Kolmogorov's phenomenological picture of an energy cascade of turbulence, although such fold characteristics still imply fluid-like deformation in the fault gouge (Wetzler et al. 2010). In order to understand the process of formation of the billow-like wavy folds, it is important to identify the temperature during seismic slip, but this has not been previously investigated for Nojima fault gouge.

Backscattered electron (BSE) observations indicate that the billow-like wavy folds consist of micrometer-sized finely comminuted grains with a lack of flow structure evidence for melting (Fig. 2c). The average volume fraction of the grains shown by pixel counting in the five squares in Fig. 2c was calculated as 0.6 with a variance (σ^2) of 0.003 using image processing software (GNU Image Manipulation Program, GIMP), whose detail data are shown in Additional file 1: Table S1.

Methods

We conducted two experiments: (1) heating experiments of fault gouge to confirm the neoformation of magnetite during heating, and (2) magnetic microscopy observations to reveal a new acquisition of remanent magnetization by neoformation of magnetite after heating and their spatial detection of heated zones.

To determine the spatial distribution of ferrimagnetic minerals in Nojima fault gouge, we used a custom-made

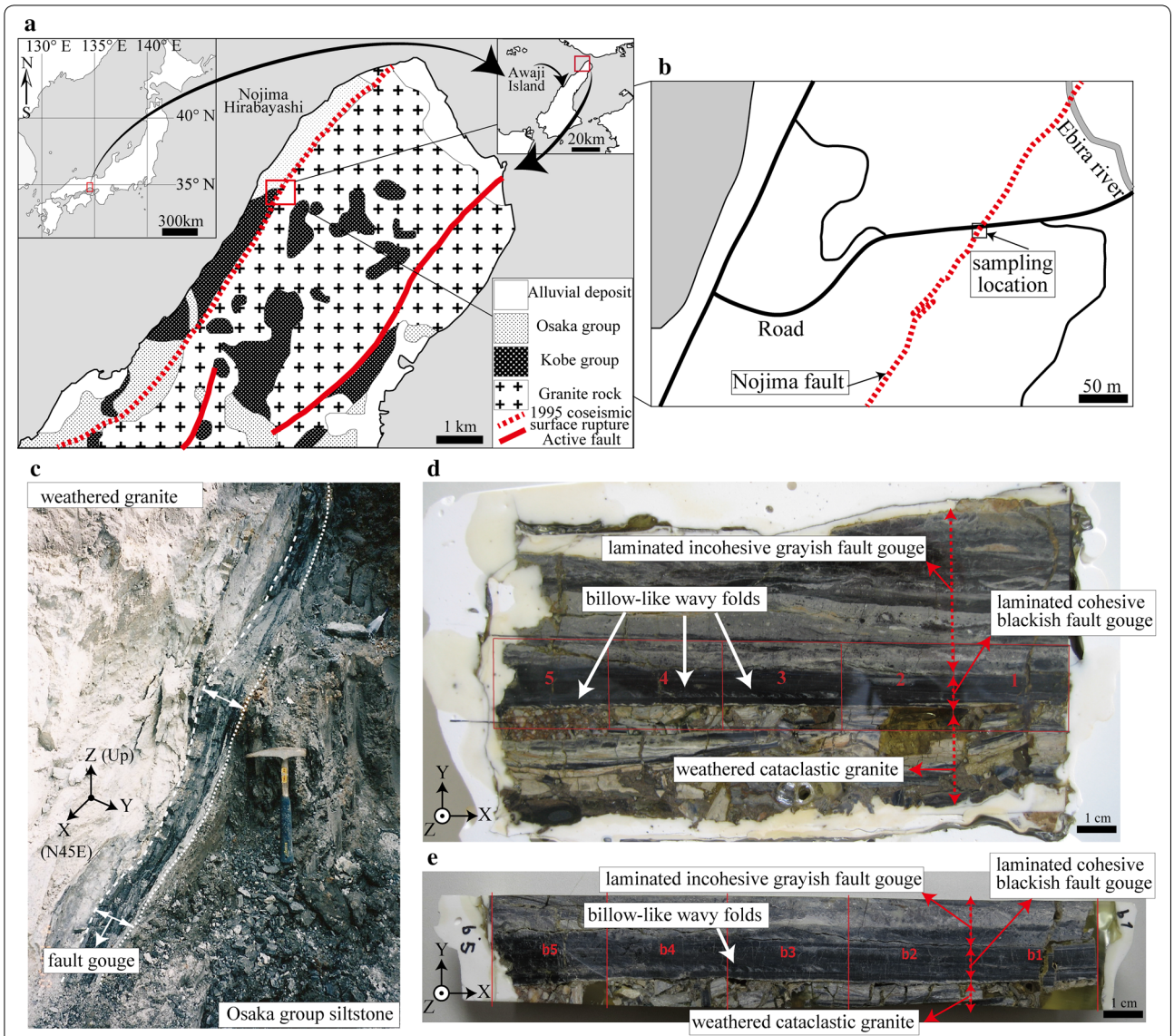

Fig. 1 **a** Location of Awaji Island, Japan, showing active faults and geology in the Kobe–Osaka area, modified after Lin et al. (2015) and Murakami et al. (2002). **b** Nojima fault gouge sampling location, modified after Otsuki et al. (2003). **c** Outcrop of the Nojima fault gouge. The fault gouge is observed between the weathered granite and the Osaka group siltstone, with *dashed* and *dotted white lines* indicating its *upper* and *lower* boundaries, respectively. The fault slip zone strikes N45°E, and dips 80° to the southeast. The *X*-axis indicates the strike and the *Z*-axis indicates up. The same *X*–*Y*–*Z* coordinate system is used in Figs. 1d, e, 2a, b, 6, and Additional file 1: S2. **d** Macroscopic photograph of the fault gouge sample used for scanning magneto-impedance (MI) magnetic microscope observation. Block samples used for making a thin section are indicated by *red numbering*. Billow-like wavy folds are observed within the laminated cohesive blackish gouge and also in between weathered granite and blackish gouge. **e** Macroscopic photograph of the fault gouge sample used for superconducting quantum interference device (SQUID) microscope observation. Block samples used for making a thin section are indicated in *red*. Billow-like wavy folds are observed within the laminated cohesive blackish gouge

scanning MI magnetic microscope developed by Uehara and Nakamura (2007, 2008). This allows mapping of the two-dimensional vertical component of a magnetic field by documenting dipole-like features with a spatial resolution of 0.4 mm with a magnetic sensitivity of 10 nT (Uehara and Nakamura 2007, 2008). The distance between the MI sensor head and the thin-section sample was about 300 μm. Since the stray magnetic field of fault gouge on thin sections was weaker than the MI sensitivity, the thin-section samples were given isothermal remanent magnetization (IRM) at 1 T by pulse magnetizer (Magnetic Measurements MMPM10) to emphasize the spatial distribution of ferrimagnetic minerals.

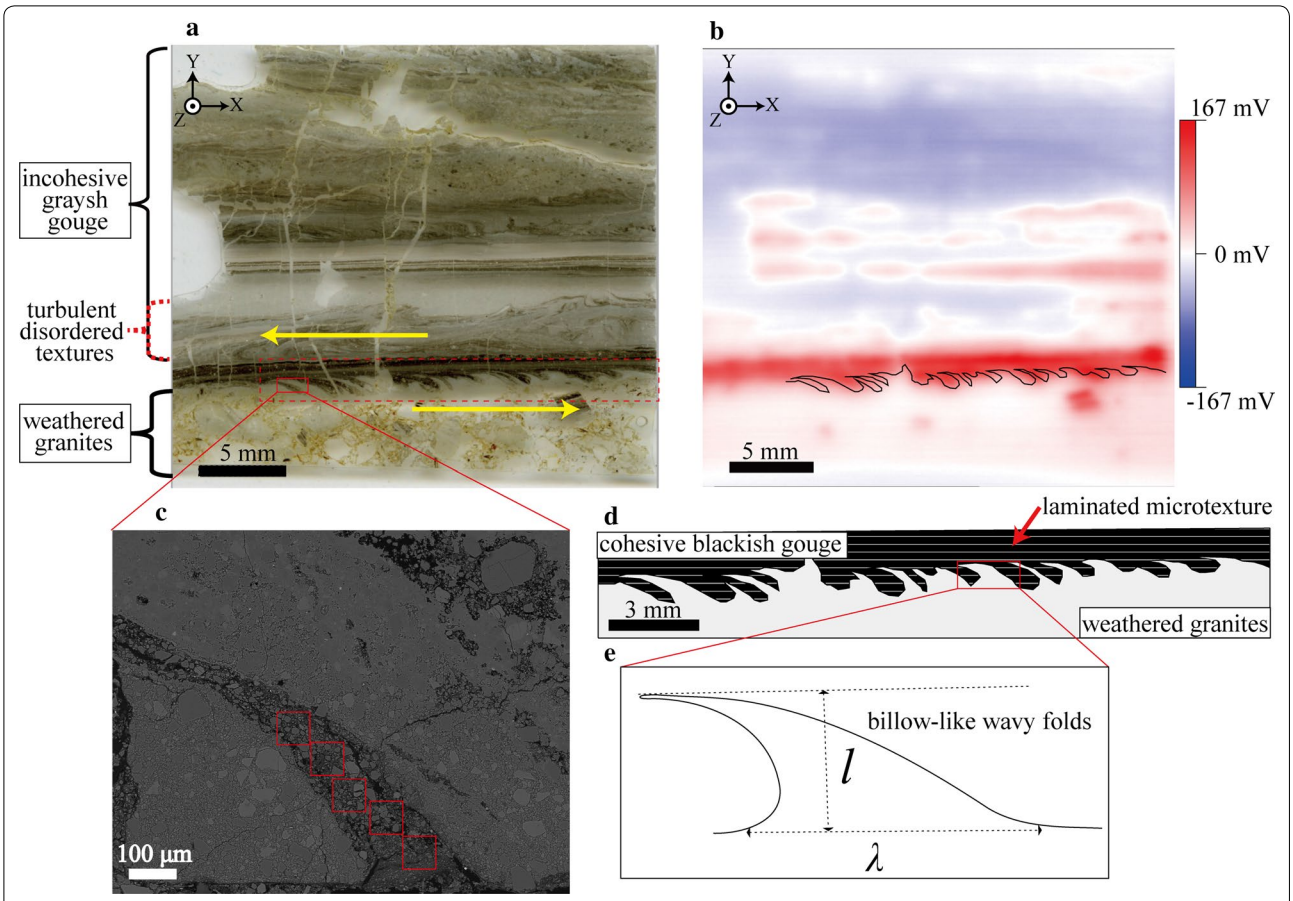

Fig. 2 **a** Optical image of a thin section from block sample 5 in Fig. 1d. The fault gouge consists of three parts, incohesive grayish gouges, cohesive blackish gouges, and weathered granites. The microstructure shows turbulent disordered textures, laminated textures, and billow-like wavy folds. **b** Surface magnetic field distribution of the thin-section sample observed under the MI magnetic microscope after imparting IRM at 1 T. *White regions* correspond to near-average magnetic field, and *red* (*blue*) regions correspond to upward (*downward*) oriented fields. The voltage is proportional to the magnetic field detected by the MI sensor. **c** Backscattered electron (BSE) image of the billow-like wavy folds in the *solid red rectangle* in (**a**). **d** Schematic of the billow-like wavy folds in the *red dashed rectangle*in (**a**), which are generated between the cohesive blackish gouge and the weathered granites. **e** Definition of width (*l*) and wavelength (λ) of the billow-like wavy folds

In order to confirm the production of ferrimagnetic mineral during high-temperature treatments, we conducted a heating experiment on the weakly magnetic incohesive grayish gouge as a starting material. Seven fault gouge samples were cut into approximately 1-cm-square fragments with an ultrasonic cutter from incohesive grayish gouge, avoiding the inclusion of magnetic blackish gouges. The samples were taken from the gouge that seemed to have not experienced high-temperature conditions during friction. Seven fragment samples were demagnetized at 100 mT using an alternating field (AF) demagnetizer (DEM-93; Natsuhara Giken, Osaka, Japan), and five of the seven were then placed in a direct current (DC) magnetic field of 100 μT thermal demagnetizer (TDF-98; Natsuhara Giken) and heated stepwise in a quartz glass tube with a low-oxygen state close to a vacuum (0.4 mbar, similar to conditions at 3 km depth). The heating steps were 100, 200, 300, 350, 400, 450, 500, 550, and 600 °C, and after each remanent, magnetization of the samples was measured using a fluxgate spinner magnetometer with a sensitivity of 5×10^{-6} mAm^2 (ASPIN; Natsuhara Giken).

To confirm that the increase in remanent magnetization of fragment samples in the previous experiments mainly stemmed from the acquisition of thermal remanent magnetization (TRM) by newly formed ferromagnetic minerals, rather than by preexisted ferromagnetic grains, we conducted the following procedure. The remaining two of the seven fragment samples were AF-demagnetized at 100 mT and acquired IRM at 1 T by a pulse magnetizer. Then, these were heated at 600 °C with a low-oxygen state (0.4 mbar, similar to conditions at

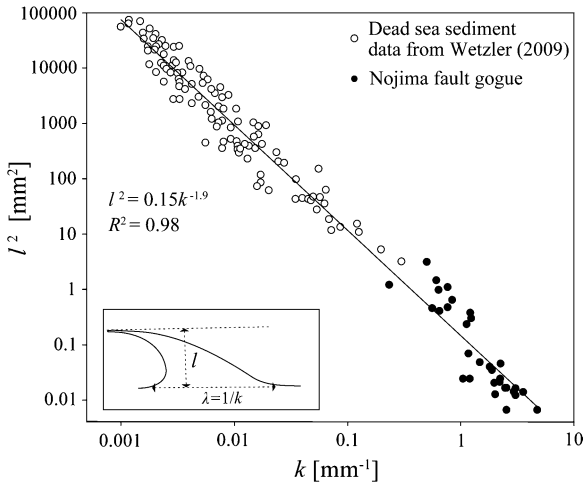

Fig. 3 Spectral distribution of deformation formed in Dead Sea sediments (*open circles* Wetzler 2009) and the billow-like wavy folds in the Nojima fault gouge (*solid circles*), where *l* is width and *k* is the inverse of the wavelength (1/λ) of the billow-like wavy folds. The *black line* is the mean power fit to the overall distribution

3 km depth) in a glass tube, and then it acquired IRM at 1 T at room temperature. Their remanent magnetizations were measured in each step using the fluxgate spinner magnetometer.

We employed the SSM at GSJ, AIST (Kawai et al. 2016; Oda et al. 2016), in order to measure the natural remanent magnetization (NRM) of the billow-like wavy folds and estimate the time of NRM acquisition. The limiting magnetic moment sensitivity of the SSM is about 1×10^{-14} A/m^2 at a sensor-to-sample distance of 200 μm (Oda et al. 2016). The measurements were taken with a distance of about 656 μm between the thin-section sample and the SQUID pickup coil.

Results and discussion

From inertial isotropic Kolmogorov turbulence power law, turbulent flow energy cascades to smaller scales with no loss of viscosity with a power law slope of −5/3. However, Li and Yamazaki (2001) observed from their fluid experiments that the power law slope at low wavenumbers is close to −2, rather than −5/3, which agrees with our plotting of data from Dead Sea sediments and billow-like wavy folds in Nojima fault gouge (Fig. 3). Considering the effect of the fluctuations in dissipation rate, the fractal dimension (*D*) of the turbulence distribution is used to describe the energy spectrum as follows: $E(k) \propto \varepsilon^{2/3}k^{-5/3}(Lk)^{-(3-D)/3}$, where $E(k)$ is the energy spectrum, ε is the dissipation rate, k is the wave number ($k = 1/\lambda$, where λ is the wavelength), and L is the maximum amplitude of turbulence (Frisch et al. 1978). If turbulence is spatially distributed, with a fractal dimension of 3, the energy spectrum becomes $E(k) \propto \varepsilon^{2/3}k^{-5/3}$, which matches the Kolmogorov turbulence power law exponent and indicates that the energy of turbulent flow is distributed to the whole volume. Our study shows that the power spectra of the Dead Sea sediment deformations and the billow-like wavy folds in Nojima fault gouge follow a similar trend with a power law fit of about −2. Therefore, we deduce a fractal dimension of 2, derived from $-5/3 - (3 - D)/3 = -2$. This indicates that the energy of turbulence tends to be distributed in a two-dimensional surface.

The remanent magnetization of the five fragment samples abruptly increased at above 350 °C, reaching levels that were about 7–26, 25–77, and 29–981 times more intense than the original remanent magnetization at 100 °C at temperatures of 400, 500, and 600 °C, respectively (Fig. 4). In all samples except Nojima 14, remanent magnetization saturated above 550 °C. To isolate the effect of thermal treatments, we compared remanent magnetization of the samples that were heated and acquired IRM at 1 T (Nojima 15: 2.13×10^2 A/m, Nojima 19: 1.52×10^1 A/m) with the ones that only acquired IRM at 1 T (Nojima 15: 1.03×10^1 A/m, Nojima 19: 2.53 A/m). The thermally treated sample acquired six times more intense remanent magnetization than non-heat-treated one (Fig. 5). This suggests the occurrence of thermal decomposition of antiferromagnetic or paramagnetic minerals into magnetite by frictional heating in seismic slip (e.g., Nakamura et al. 2002). The production of magnetite by a thermal decomposition was confirmed in thermomagnetic experiments of incohesive grayish fault gouge (see Additional file 1: Fig. S3). Using our MI magnetic microscope, a stray magnetic field distribution of the billow-like folds in the fault gouge in an isothermally magnetized state shows that the cohesive blackish gouges and the billow-like wavy folds are strongly magnetized, while the weathered granites are weakly or null magnetized (Fig. 2b; Additional file 1: Fig. S2). This suggests that these strongly magnetized slip zones had been exposed to high temperature (>350 °C).

Chou et al. (2012) also suggested that newly formed ferrimagnetic mineral in Taiwan Chelungpu fault gouge records Earth's magnetic field during the post-seismic period as a NRM. This implies the possibility to determine the age of ancient frictional heating. However, our MI magnetic microscope is not able to detect weakly magnetized fault gouge. To capture the NRM distribution in fault gouges, we need to use a high-sensitivity SSM. The NRM magnetic field distribution of the Nojima fault gouge shows that the blackish gouge adjacent to the billow-like wavy fold was strongly magnetized in opposite directions (Fig. 6). Our results show that a SSM can detect the NRM distribution of fault

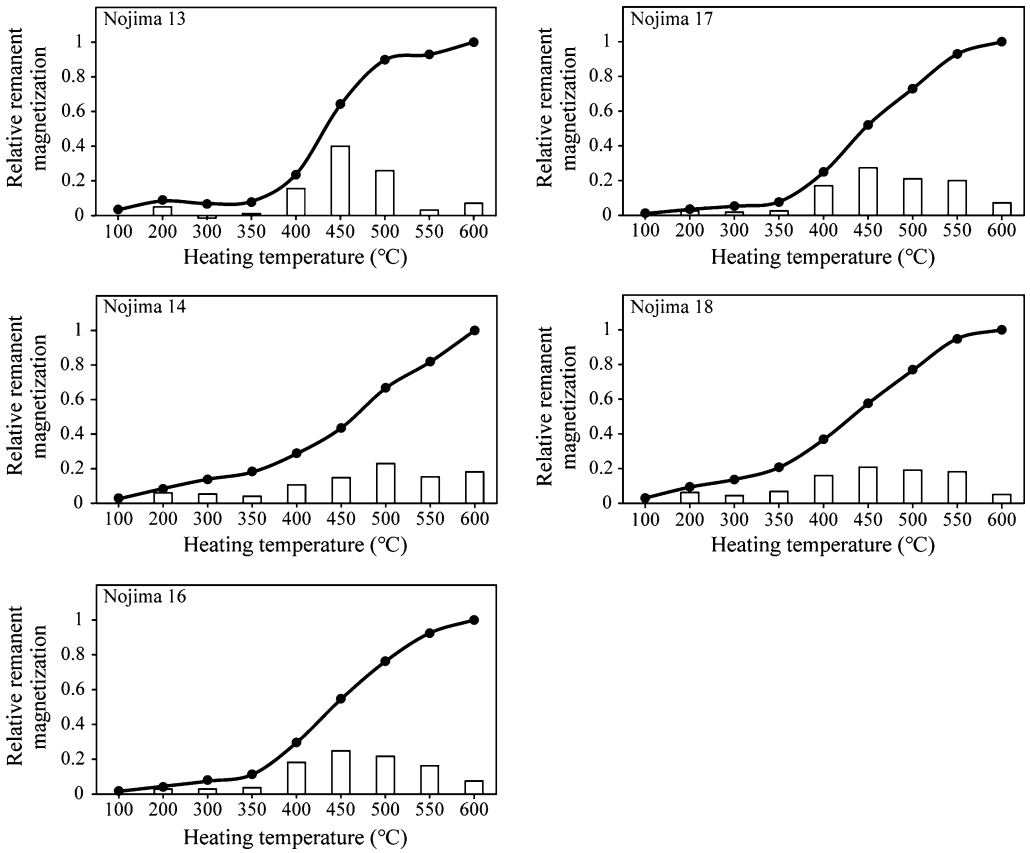

Fig. 4 Relative remanent magnetization of the five fragment gouge samples after stepwise heating experiment at 100 μT, normalized with respect to maximum magnetization at 600 °C. The histograms show the amount of partial remanent magnetization acquired during heating (e.g., at 400 °C, the histogram indicates the amount of remanent magnetization acquired between 350 and 400 °C). The raw data are shown in Additional file 1: Table S2

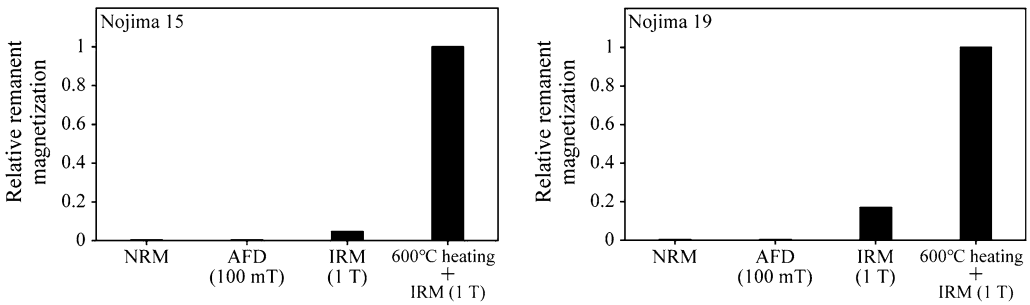

Fig. 5 Relative remanence magnetization of two fragment gouge samples under natural remanent magnetization (NRM), alternating field demagnetization (AFD) at 100 mT, isothermal remanent magnetization (IRM) at 1 T and IRM at 1 T after heating at 600 °C. The raw data are shown in Additional file 1: Table S3

gouge (Fig. 6), and the patterns of positively and negatively magnetized states seem to be due to geomagnetic polarity reversals. These patterns are related to the slip zone and the billow-like wavy folds of the fault gouge. This suggests that the NRM distribution of fault gouge may allow us to date frictional slips using a geomagnetic polarity timescale.

From our fault gouge heating experiments and scanning MI magnetic microscope observations, we hypothesized that the cohesive blackish gouges are the fault slip zone

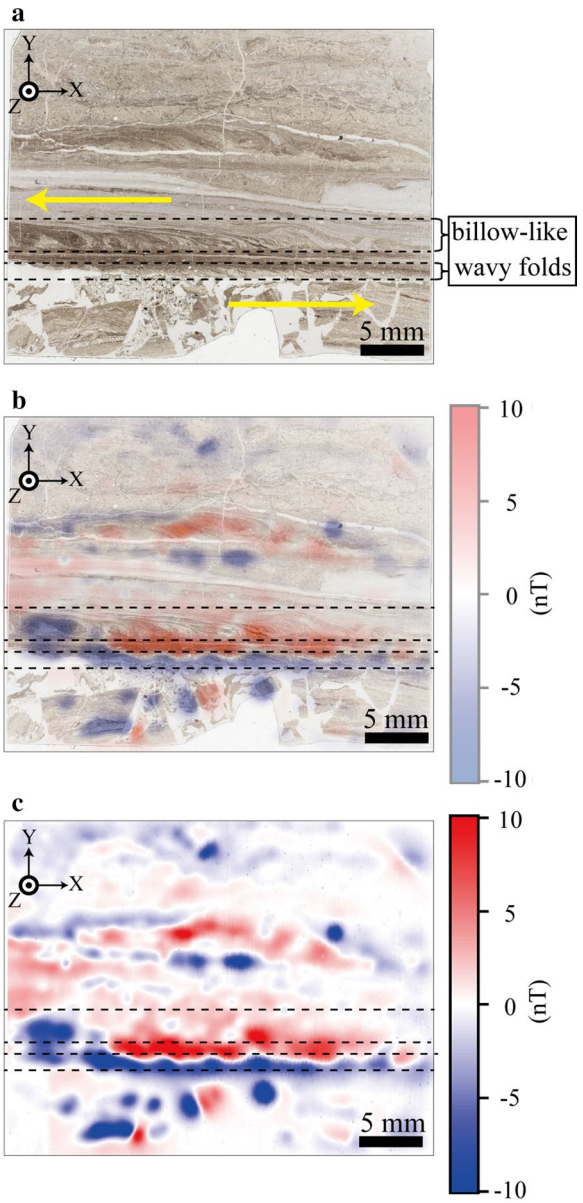

Fig. 6 **a** Optical image of a thin section from block sample b3 in Fig. 1e. The *yellow arrow* indicates a direction of fault movement estimated from the billow-like wavy folds. **b** A semitransparent SQUID microscopic image superimposed on the optical image. **c** A SQUID microscopic image of the thin section. Positive (negative) magnetic field values correspond to upward (downward) oriented fields

and reached 350 °C at least. The maximum attainment temperature of the fault slip zone can be determined from the aspects of the BSE image and the billow-like wavy folds caused by KH instability. Otsuki et al. (2003) indicated that Nojima fault gouge underwent local melting or fluidization and that the melt viscosity changed from 10^{7-9} Pa s at 750–800 °C to 10 Pa s at 1280 °C. However, they suggested that the phase transition from a grain friction regime to fluidization of granular materials could be achieved, if the temperature of frictional heating does not reach the fault gouge melting point. At that time, relative viscosity [the ratio of total fluid viscosity (η_s) to the pore fluid viscosity (η_m)] is about 100, if the volume fraction of an equivalent diameter spherical particle (N) is 0.6 (Frith et al. 1996). We hypothesized that the fault slip zone was exposed to high temperature (>350 °C) and that the fault gouge formation depth was 3 km. Under such temperature and pressure conditions, Schmelzer et al. (2005) showed that the viscosity of water [pore fluid (η_m)] is 9.137×10^{-5} Pa s, being approximately 1.0×10^{-4} Pa s. Therefore, if micrometer-sized finely comminuted products approximate to an equivalent diameter spherical particle, total viscosity (η_s) is 1.0×10^{-2} Pa s. Due to frictional heating, the pore fluid expands in volume (e.g., Lachenbruch 1980). If the permeability of the fault slip zone decreases, the volume fraction of fault gouge decreases; this suggests that the total fluid viscosity of the fault slip zone further reduces below 1.0×10^{-2} Pa s. Although Woods (1969) has demonstrated that KH instability can be generated under high Reynolds number conditions, we cannot deduce the concrete Reynolds number due to the difficulty in the estimation of the flow velocity in fault gouge. With regard to shear flow, viscosity dissipates disturbance energy and stabilizes the flow. The viscosity of fluid in the fault gouge caused by fluidization is much lower than that associated with melting, which suggests that fluidization is a more appropriate condition for the generation of KH instability; this is supported by the BSE observations showing that the folds consist of micrometer-sized finely comminuted grains without flow structures. This finding suggests that the low-viscosity fluid and frictional heating decreased the frictional strength of the fault gouge, and that the temperature was below its melting point of 750 °C. Monazam et al. (2014) demonstrated that the oxidation of magnetite to hematite was terminated at 900 °C within a minute in a continuous stream of air. Although the experimental conditions are different from those in the Nojima fault, it is considered that the oxidation of magnetite to hematite did not occur during ancient seismic slips in our case. This result supports that magnetite was formed in the fault slip zone around the billow-like wavy folds because of frictional heating below 900 °C during seismic slip, which contributes strong remanent magnetization. Therefore, frictional heating between the fault grains occurred in seismic slip and generated magnetite. After that, the low viscous fluid composed of water and the fault grains induced by fluidization decreased the frictional strength of the fault slip zone. During a frictional slip, the velocity difference in viscous fluids formed magnetized billow-like wavy folds due to KH instability, and the microtexture had been preserved in fault gouge after the cease of an ancient seismic slip.

Conclusion

In Nojima fault gouge, we found billow-like wavy folds which are similar in form to Kelvin–Helmholtz (KH) instabilities. Scanning magnetic microscope using MI and SQUID sensors detected the presence of magnetic minerals in the slip zone surrounding the billow-like wavy fold. The rock magnetic studies show that the magnetic mineral was formed as a result of thermal decomposition (>350 °C) of antiferromagnetic or paramagnetic mineral into magnetite during frictional slips. BSE observations indicated the billow-like wavy folds consisted of micrometer-sized finely comminuted grains without flow structures associated with melting. These results suggest that fluidization induced by fault rupture and frictional heating was the driving mechanism of fault lubrication.

Additional file

Additional file 1: Fig. S1. Transmitted light microscope images of thin-section samples with billow-like wavy folds in their laminated microtextures. Dashed red lines outline the billow-like wavy folds, and dashed black dot lines indicate width (*l*) and the wavelength (λ). **Fig. S2.** Optical images (left) and surface magnetic field distributions observed by MI magnetic microscope (right) of thin-section samples shown in the relative intensity map. Dotted black lines indicate the billow-like wavy folds. White regions correspond to near-average magnetic field, and red (blue) regions correspond to upward (downward) oriented fields. The black arrow indicates a direction of fault movement estimated from the billow-like wavy folds. (a), (b), and (c) correspond to blocks 1, 2, and 4 in Fig. 1d, respectively. **Fig. S3.** Thermomagnetic curves of incohesive grayish fault gouge samples (a) and a subsequent heating curve (b). The curve (a) was characterized by hump above 370 °C. The induced magnetization on a heating step increases at about 370 °C, reached a maximum at 500 °C, and decreases from 500 °C to 570 °C. This hump suggests the presence of thermally unstable iron-bearing minerals that can be transformed to magnetite at temperature above 370 °C. The subsequent heating curve (b) showed that the induced magnetization decreases to the Curie temperature of around 550 °C and increases reversibly back to the same level of original magnetization. This indicates the existence of magnetite without thermal oxidations to hematite even after heating up to 650 °C. **Table S1.** Relationship between pixel counting and volume fraction of fault grains. **Table S2.** Raw data of remanent magnetization of the five fragment gouge samples after stepwise heating experiment at 100 μT. **Table S3.** Raw data of remanence magnetization of two fragment gouge samples under natural remanent magnetization (NRM), alternating field demagnetization (AFD) at 100 mT, isothermal remanent magnetization (IRM) at 1 T and IRM at 1 T after heating at 600 °C.

Abbreviations

AIST: National Institute of Advanced Industrial Science and Technology; AF: alternating field; BSE: backscattered electron; CRM: chemical remanent magnetization; DC: direct current; ESR: electron spin resonance; GSJ: Geological survey of Japan; IRM: isothermal remanent magnetization; KH: Kelvin–Helmholtz; MI: magneto-impedance; NRM: natural remanent magnetization; SQUID: superconducting quantum interference device; SSM: Scanning SQUID microscope; TRM: thermal remanent magnetization.

Authors' contributions

TF conceived the study, processed and interpreted the data, and drafted the manuscript. NN conceived the study, processed and interpreted the data, and provided critical revisions of the draft manuscript. HO contributed to SSM measurements and data calibration. MU contributed to scanning MI magnetic microscope measurements and drafted the manuscript. HN evaluated the analytical procedure and drafted the manuscript. All authors read and approved the final manuscript.

Author details

[1] Department of Earth Science, Tohoku University, Sendai, Japan. [2] Institute for Excellence in Higher Education, Tohoku University, Sendai, Japan. [3] Geological Survey of Japan, Research Institute of Geology and Geoinformation, AIST, Tsukuba, Japan. [4] CNRS, Aix Marseille Univ, IRD, Coll France, CEREGE, Aix-en-Provence, France.

Acknowledgements

We would like to thank Dr. Kenshiro Otsuki for helping in the field collection of Nojima fault gouge samples. We acknowledge the critical review comments by Dr. Eric Ferré and an anonymous reviewer. We would like to thank Dr. Jun Kawai of the Appl. Electron. Lab., Kanazawa Inst. of Technol., Kanazawa, Japan, for setting up the SSM and Ms. Ayako Katayama of the Geological Survey of Japan, Research Institute of Geology and Geoinformation, AIST, Tsukuba, Japan, for helping with SSM measurements. This study was performed using high-temperature vibrating magnetometer of National Institute of Polar Research (NIPR) through General Collaboration Project No. 25-18. We made map (Fig. 1) with ArcGIS software (ESRI Inc., www.esri.com). We received generous support from Mr. Michiaki Abe at Tohoku University (Sendai, Japan) in the making of thin-section samples. This work was supported by the Japan Society for the Promotion of Science Grant-in-Aid for Scientific Research (B) (Grant Nos. 22340146 and 15H02986) and of Science Grant-in-Aid for Scientific Research (A) (Grant No. 25247073).

Competing interests

The authors declare that they have no competing interests.

Publisher's Note

Received: 20 January 2017 Accepted: 6 April 2017
Published online: 18 April 2017

References

Allen AR (1979) Mechanism of frictional fusion in fault zones. J Struct Geol 1:231–243. doi:10.1016/0191-8141(79)90042-7

Awata Y, Mizuno K, Sugiyama Y, Imura R, Shimokawa K, Okumura K, Tsukuda E (1996) Surface fault ruptures on the northeast coast of Awaji Island associated with the Hyogo-ken Nanbu earthquake of 1995, Japan. J Seismol Soc Jpn 49:113–124 **(in Japanese with English abstract)**

Boullier AM, Yeh EC, Boutareaud S, Song SR, Tsai CH (2009) Microscale anatomy of the 1999 Chi-Chi earthquake fault zone. Geochem Geophys Geosyst 10:Q03016. doi:10.1029/2008GC002252

Brodsky EE, Rowe CD, Meneghini F, Moore JC (2009) A geological fingerprint of low-viscosity fault fluids mobilized during an earthquake. J Geophys Res 114:B01303. doi:10.1029/2008JB005633

Cardwell RK, Chinn DS, Moor GF, Turcotte DL (1978) Frictional heating on a fault zone with finite thickness. Geophys J R Astron Soc 52:525–530. doi:10.1111/j.1365-246X.1978.tb04247.x

Chou YM, Song SR, Aubourg C, Lee TQ, Boullier AM, Song YF, Yeh EC, Kuo LW, Wang CY (2012) An earthquake slip zone is a magnetic recorder. Geology 40:551–554. doi:10.1130/G32864.1

Di Toro G, Han R, Hirose T, De Paola N, Nielsen S, Mizoguchi K, Ferri F, Cocco M, Shimamoto T (2011) Fault lubrication during earthquakes. Nature 471:494–499. doi:10.1038/nature09838

Dunlop DJ, Özdemir Ö (1997) Rock magnetism: fundamentals and frontiers. Cambridge University Press, Cambridge

Enomoto Y, Zheng Z (1998) Possible evidences of earthquake lightning accompanying the 1995 Kobe Earthquake inferred from the Nojima fault gouge. Geophys Res Lett 25:2721–2724. doi:10.1029/98GL02015

Ferré EC, Zechmeister MS, Geissman JW, MathanaSekaran N, Kocak K (2005) The origin of high magnetic remanence in fault pseudotachylites: theoretical considerations and implication for coseismic electrical currents. Tectonophys 402:125–139. doi:10.1016/j.tecto.2005.01.008

Ferré EC, Geissman JW, Demory F, Gattacceca J, Zechmeister MS, Hill MJ (2014) Coseismic magnetization of fault pseudotachylytes: 1. Thermal demagnetization experiments. J Geophys Res Solid Earth 119:6113–6135. doi:10.1002/2014JB011168

French BM (1971) Stability relations of siderite ($FeCO_3$) in the system Fe–CO. Am J Sci 271:37–78

Frisch U, Sulem PL, Nelkin M (1978) A simple dynamical model of intermittent fully developed turbulence. J Fluid Mech 87:719–736. doi:10.1017/S0022112078001846

Frith WJ, d'Haene P, Buscall R, Mewis J (1996) Shear thickening in model suspensions of sterically stabilized particles. J Rheol 40:531–548. doi:10.1122/1.550791

Fukuchi T (2003) Strong ferrimagnetic resonance signal and magnetic susceptibility of the Nojima pseudotachylyte in Japan and their implication for coseismic electromagnetic changes. J Geophys Res 108:2312. doi:10.1029/2002JB002007

Fukuchi T (2012) ESR techniques for the detection of seismic frictional heat. Earthquake research and analysis—seismology, seismotectonic and earthquake geology. InTech, Rijeka, pp 317–340. doi:10.5772/28061

Fukuchi T, Mizoguchi K, Shimamoto T (2005) Ferrimagnetic resonance signal produced by frictional heating: a new indicator of paleoseismicity. J Geophys Res 110:B12404. doi:10.1029/2004JB003485

Helmholtz H (1868) Über diskontinuierliche Flüssigkeits-Bewegungen. Monatsbericht der königlich preussischen Akademie der Wissenschaften zu Berlin 23:215–228. Translated into English by F. Guthrie (1868) On discontinuous movements of fluids. Phil Mag 36:337–46

Hirono T, Ikehara M, Otsuki K, Mishima T, Sakaguchi M, Wonn S, Omori M, Lin W, Yeh EC, Tanikawa W, Wang CY (2006) Evidence of frictional melting from disk-shaped black material, discovered within the Taiwan Chelungpu fault system. Geophys Res Lett 33:L19311. doi:10.1029/2006GL027329

Jeffreys H (1942) On the mechanics of faulting. Geol Mag 79:291–295. doi:10.1017/S0016756800076019

Kameda J, Matsugi H, Tanaka H (2002) Occurrence of Pseudotachylyte obtained from the Nojima fault at Nojima–Hirabayashi, Awaji Island, Japan. J Geol Soc Jpn 4:IX–X. doi:10.5575/geosoc.108.IX

Kawai J, Oda H, Fujihira J, Miyamoto M, Miyagi I, Sato M (2016) SQUID microscope with hollow-structured cryostat for magnetic field imaging of room temperature samples. IEEE Trans Appl Supercond 26:1600905. doi:10.1109/TASC.2016.2536751

Kelvin L (1871) Hydrokinetic solutions and observations. Phil Mag 42(4):362–377

Lachenbruch AH (1980) Frictional heating, fluid pressure, and the resistance to fault motion. J Geophys Res 85:6097–6122. doi:10.1029/JB085iB11p06097

Li H, Yamazaki H (2001) Observations of a Kelvin–Helmholtz billow in the ocean. J Oceanogr 57:709–721. doi:10.1023/A:1021284409498

Lin A, Katayama S, Rao G, Kubota Y (2015) Structural analysis of a previously unknown active fault that triggered the 2013 Mw 5.8 Awajishima Earthquake, southwest Japan. Bull Seismol Soc Am 105:1169–1178. doi:10.1785/0120140122

Maekawa Y, Hirono T, Yabuta H, Mukoyoshi H, Kitamura M, Ikehara M, Tanikawa W, Ishikawa T (2014) Estimation of slip parameters associated with frictional heating during the 1999 Taiwan Chi-Chi earthquake by vitrinite reflectance geothermometry. Earth Planets Space 66:28. doi:10.1186/1880-5981-66-28

Mase CW, Smith L (1984) Pore-fluid pressures and frictional heating on a fault surface. Pure appl Geophys 122:583–607. doi:10.1007/BF00874618

Mase CW, Smith L (1987) Effects of frictional heating on the thermal, hydrologic, and mechanical response of a fault. J Geophys Res 92:6249–6272. doi:10.1029/JB092iB07p06249

McKenzie DP, Brune JN (1972) Melting on fault planes during large earthquakes. Geophys J R Astron Soc 29:65–78. doi:10.1111/j.1365-246X.1972.tb06152.x

Mishima T, Hirono T, Soh W, Song S (2006) Thermal history estimation of the Taiwan Chelungpu fault using rock-magnetic methods. Geophys Res Lett 33:L23311. doi:10.1029/2006GL028088

Mishima T, Hirono T, Nakamura N, Tanikawa W, Soh W, Song S (2009) Changes to magnetic minerals caused by frictional heating during the 1999 Taiwan Chi-Chi earthquake. Earth Planets Space 61:797–801. doi:10.1186/BF03353185

Mizoguchi K, Hirose T, Shimamoto T, Fukuyama E (2009) High-velocity frictional behavior and microstructure evolution of fault gouge obtained from Nojima fault, southwest Japan. Tectonophys 471:285–296. doi:10.1016/j.tecto.2009.02.033

Monazam ER, Breault RW, Siriwardane R (2014) Kinetics of magnetite (Fe_3O_4) oxidation to hematite (Fe_2O_3) in air for chemical looping combustion. Ind Eng Chem Res 53:13320–13328. doi:10.1021/ie501536s

Monzawa N, Otsuki K (2003) Comminution and fluidization of granular fault materials: implications for fault slip behavior. Tectonophys 367:127–143. doi:10.1016/S0040-1951(03)00133-1

Murakami M, Tagami T, Hasebe N (2002) Ancient thermal anomaly of an active fault system: zircon fission-track evidence from Nojima GSJ 750 m borehole samples. Geophys Res Lett 29:2123. doi:10.1029/2002GL015679

Nakamura N, Hirose T, Borradaile GJ (2002) Laboratory verification of submicron magnetite production in pseudotachylytes: relevance for paleointensity studies. Earth Planet Sci Lett 201:13–18. doi:10.1016/S0012-821X(02)00704-5

Oda H, Kawai J, Miyamoto M, Miyagi I, Sato M, Noguchi A, Yamamoto Y, Fujihira J, Natsuhara N, Aramaki Y, Masuda T, Xuan C (2016) Scanning SQUID microscope system for geological samples: system integration and initial evaluation. Earth Planets Space 68:179. doi:10.1186/s40623-016-0549-3

Oshiman N, Shimamoto T, Takemura K, Wibberley CAJ (2001) Thematic issue: Nojima fault zone probe. Island Arc 10:195–505. doi:10.1111/j.1440-1738.2001.00350.x

Otsuki K, Minagawa J, Aono M, Ohtake M (1997) On the curved striations of Nojima seismic fault engraved at the 1995 Hyogoken–Nambu earthquake. J Seismol Soc Jpn 49:451–460 **(in Japanese with English abstract)**

Otsuki K, Monzawa N, Nagase T (2003) Fluidization and melting of fault gouge during seismic slip: identification in the Nojima fault zone and implications for focal earthquake mechanisms. J Geophys Res 108:2192. doi:10.1029/2001JB001711

Piper JDA, Poppleton TJ (1988) Palaeomagnetic dating of pseudotachylyte formation in the Lewisian complex. Scott J Geol 24:263–272. doi:10.1144/sjg24030263

Savage HM, Polissar JP, Sheppard R, Rowe DC, Brodsky EE (2014) Biomarkers heat up during earthquakes: new evidence of seismic slip in the rock record. Geology 42:99–102. doi:10.1130/G34901.1

Schmelzer PWJ, Zanotto DE, Fokin MV (2005) Pressure dependence of viscosity. J Chem Phys 122:074511. doi:10.1063/1.1851510

Sibson RH (1973) A mechanism for partial or total stress relief. Nature 243:66–68. doi:10.1038/physci243066a0

Sibson RH (1975) Generation of pseudotachylyte by ancient seismic faulting. Geophys J R Astron Soc 43:775–794. doi:10.1111/j.1365-246X.1975.tb06195.x

Uda S, Lin A, Takemura K (2001) Crack-filling clays and weathered cracks in the DPRI 1800 m core near the Nojima Fault, Japan: evidence for deep surface-water circulation near an active fault. Island Arc 10:439–446. doi:10.1111/j.1440-1738.2001.00342.x

Uehara M, Nakamura N (2007) Scanning magnetic microscope system utilizing a magneto-impedance sensor for a nondestructive diagnostic tool of geological samples. Rev Sci Instrum 78:043708. doi:10.1063/1.2722402

Uehara M, Nakamura N (2008) Identification of stable remanence carrier through a magneto-impedance (MI) scanning magnetic microscope. Stud Geophys Geod 52:211–223. doi:10.1007/s11200-008-0014-2

Ujiie K, Yamaguchi A, Kimura G, Toh S (2007) Fluidization of granular material in a subduction thrust at seismogenic depths. Earth Planet Sci Lett 259:307–318. doi:10.1016/j.epsl.2007.04.049

Wetzler N (2009) Examination of Kelvin–Helmholtz instability as a mechanism of deformation in the Lisan Formation, Dead Sea Basin. MSc Thesis, Tel Aviv Univ

Wetzler N, Marco S, Heifetz E (2010) Quantitative analysis of seismogenic shear-induced turbulence in lake sediments. Geology 38:303–306. doi:10.1130/G30685.1

Woods DJ (1969) On Richardson's number as a criterion for laminar–turbulent–laminar-transition in the ocean and atmosphere. Radio Sci 4:1289–1298. doi:10.1029/RS004i012p01289

Yoshikawa S (1973) The Osaka Group in the southeast of Osaka. J Geol Soc Jpn 79:33–45. doi:10.5575/geosoc.79.33 **(in Japanese)**